TEM cell for Testing Low-profile Integrated Circuits for EMC

Alexander V. Demakov, Maxim E. Komnatnov, *Member IEEE*
Tomsk State University of Control Systems and Radioelectronics,
Tomsk, Russia

Abstract – **The paper presents the results of development of TEM cell with a working volume of 30×30×5 mm³ for measuring radiated immunity and electromagnetic emissions of low-profile integrated circuits. A solid model of the TEM cell was developed based on the analysis of various designs for matching transitions using analytical estimation and electrodynamic simulation. A research prototype of the cell was built and its *S*-parameters measurements were performed.**

Index Terms – **TEM cells, integrated circuit noise, electromagnetic modeling, electromagnetic compatibility.**

I. Introduction

DEVELOPMENT trends of a modern semiconductor electronic component base used in the design of various radioelectronic equipment are aimed to reducing energy consumption, increasing speed and fault tolerance. The shift towards submicron technologies for producing semiconductor elements allows increasing the operating frequencies of integrated circuits (ICs), but at the same time their supply voltages decrease [1], which leads to an increase in electromagnetic emissions at high frequencies [2] and an increase in susceptibility of radioelectronic equipment to external electromagnetic effects [3]. The reliability of radioelectronic equipment based on modern ICs can be ensured through their trouble-free operation. In this regard, it is relevant to develop methods and devices for studying and testing electronic components in order to reduce their radiation levels and susceptibility to the electromagnetic field [4].

II. Problem Statement

At present, there are a number of studies into various mechanisms of IC failure occurring under the effect of a powerful electromagnetic field, which results in degradation, damage, and disruption of the IC performance. Different studies and tests of radiated immunity of ICs demonstrate that the most intense current amplitudes are induced on conductors in resonant structures whose dimensions are close to half the wavelength when they are oriented relative to the direction of the polarization vector of the electromagnetic field [3]. In addition, the critical characteristics of radiation include the carrier frequency, energy flux density, duration and frequency of exposure, polarization and the angle of incidence of the electromagnetic field [5].

To reproduce electromagnetic interference, a direct power injection method is used, which is based on feeding the signal from the generator of radio pulses to the pin of the IC [6]. However, ICs are located on printed circuit boards (PCB) which include current-carrying printed conductors of various lengths, as well as other components necessary for the IC operation. They have a direct effect on the waveform and amplitude of the interference. A method for testing electromagnetic emission [7] and radiated immunity [8] of ICs in the TEM cell has been widely used. The design of the cell is based on the transmission line in the form of a shielded stripline segment with air dielectric filling, which is matched with connectors by means of pyramidal transitions. When the signal from the generator with the given characteristics is fed to the input connector of the cell, a TEM-wave propagates in its internal space, forms a uniform field in the working volume and is absorbed by the matched load installed on the output connector. The radiated immunity testing is carried out by placing the device under test (DUT) in the regular part of the cell and exposing it to the electromagnetic field with the required electric field strength. The average linear dimensions of modern integrated circuit packages do not exceed 30 mm with the height of no more than 5 mm, which, together with the use of case metallization and a large number of pins, leads to an increase in the electromagnetic emission of ICs in the SHF range [9]. In this regard, it is important to improve TEM cells for testing ICs in a wider frequency range.

The aim of this work is to develop a research prototype of a TEM cell with a working volume of 30×30×5 mm³ for testing ICs in the frequency range of up to 5.3 GHz.

III. Analytical Estimation Of Geometric Parameters

It is known that the operating frequency range of a TEM cell is limited by the critical frequency of the TE_{10} mode, which is determined by the geometric dimensions of the cell. According to experimental estimates [10], the DUT height should be no more than 1/3 of the distance between the base of the cell enclosure and the central conductor. This condition is necessary in order to minimize the field inhomogeneity (the required is ±3 dB), which occurs when the DUT is placed inside the cell (Fig. 1).

978-1-7281-6846-3/20/$31.00 ©2020 IEEE

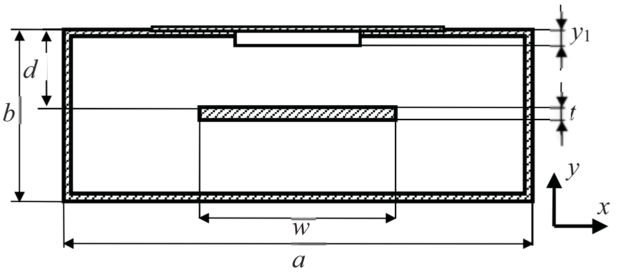

Fig. 1. Cross-section of TEM cell with the DUT.

For calculations, we chose the height of typical ICs that did not exceed $y_1 = 5$ mm. The distance between the base of the cell enclosure and the center conductor is $d = 15$ mm, and its thickness is $t = 1$ mm. With these values, the height of the regular part of the cell is $b = 31$ mm (Fig. 1). Using the formula for a shielded stripline with a rectangular cross-section and air filling [11], we calculated the dependences of the characteristic impedance Z_0 in the cross-section of the TEM cell on the ratio of the width of the central conductor to the width of the cell enclosure w/a for different a/b ratios (Fig. 2).

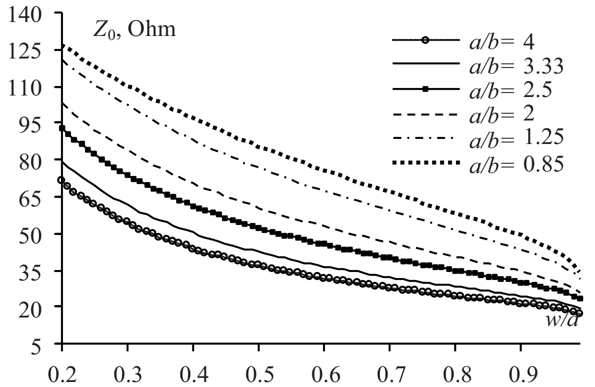

Fig. 2. Dependences of the characteristic impedance Z_0 on the ratio w/a for different a/b.

The values of width of the central conductor w and width of the enclosure a were selected taking into account the required characteristic impedance ($Z_0 = 50$ Ohm), the dimensions of the test PCB (100×100 mm^2 with metallization at the edges of the board) and the dimensions of the IC package, and basing on the ratios $a/b = 3.33$; $w/a = 0.4$; $a = 100$ mm; $w = 40$ mm.

IV. Electrodynamic Modeling

Based on the obtained geometric parameters, the development and analysis of the electrodynamic model of the regular part of the cell with a length of $L = 100$ mm were performed. Fig. 3 shows the calculated frequency dependence of the reflection coefficient magnitude $|S_{11}|$. It can be seen that the value of $|S_{11}|$ does not exceed -55 dB in the frequency range of up to 6 GHz, which indicates the matching of the regular part of the cell with a 50 Ohm feeder.

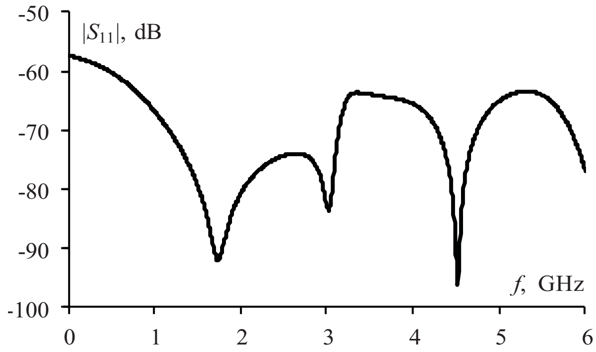

Fig. 3. Frequency dependence of $|S_{11}|$ of the regular part of the TEM cell.

To match the regular part of the TEM cell with the impedance of the coaxial connector, we considered various forms of coaxial-strip transitions. Initially, we performed the analysis of the classical design of a TEM cell with pyramidal transitions. The geometric dimensions of all elements of the construction (Fig. 4) were selected basing on experimental estimates and analytical equations from [12, 13].

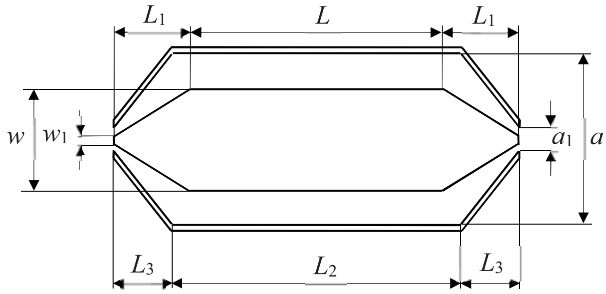

Fig. 4. Longitudinal section of the TEM cell model with pyramidal transitions.

The length of the pyramidal transition was obtained ($L_3 = 50$ mm), and the enclosure height at the location of the coaxial connectors was chosen equal to $b_1 = 4.5$ mm. The choice of this size is explained by the use of the SMA connectors with the diameters of the dielectric and the central conductor equal to 4.1 mm and 1.28 mm, respectively (the dielectric material is Teflon, $\varepsilon_r = 2.1$) to connect the cell. The values of the width of the enclosure a_1 and the central conductor w_1 at the place of the connector are selected basing on the requirements for providing $Z_0 = 50$ Ohm with the aspect ratios $a/b = a_1/b_1$ as $a_1 = 15$ mm, $w_1 = 3.9$ mm.

Next, we performed the analysis of the TEM cell model with a rectangular enclosure (Fig. 5). The dimensions of the internal volume of the enclosure were 100×100×30 mm^3, with the central conductor located inside.

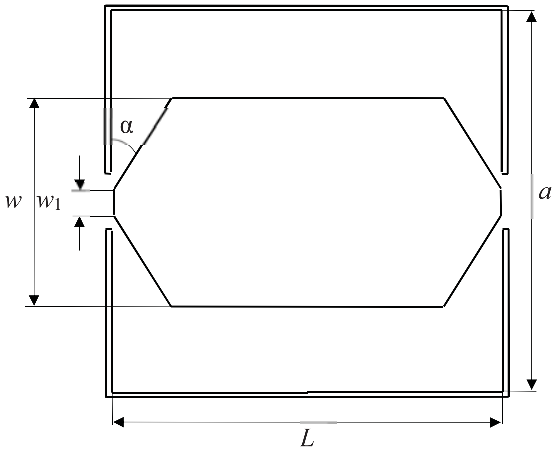

Fig. 5. Longitudinal section of the TEM cell model with a rectangular enclosure.

The narrowing angle of the central conductor width α was chosen using the trust region method [14]. As a minimized objective optimization function, we chose the maximum value of the reflection coefficient $|S_{11}|$ in the frequency range of up to 5 GHz. Basing on the optimization results, a narrowing angle α was obtained equal to 19.4°.

To expand the operating frequency band, we considered a TEM cell with a tapering enclosure width at a constant height [15, 16]. The reduction in the width of the enclosure was made at a linear angle α with a rectangular protrusion at the narrowing end. Inside it there is a circular hole for the coaxial connector, the central conductor of which is closed on the central plate of the cell. The width of the central conductor was reduced at an angle α_1 and at a distance L_1 from the longitudinal plane of the cell symmetry, and at an angle α_2 to the junction of the central conductor with the coaxial connector, as well as with rounding the corners with radii R_1 and R_2, respectively (Fig. 6).

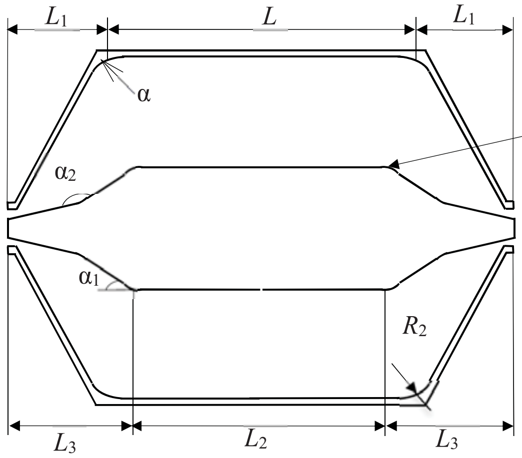

Fig. 6. Longitudinal section of the TEM cell model with a tapering enclosure width at a constant height.

The parametric optimization of this model is performed similarly to the optimization of the TEM cell with a rectangular enclosure. As a result, the following values were obtained: α = 11.9°, α_1 = 31.8°, α_2 = 136.7°, L_1 = 12.6 mm, R_1 = 2.45 mm, R_2 = 1 mm.

From the simulation results we can see that without additional design changes, $|S_{11}|$ of the TEM cell with pyramidal transitions was less than minus 20 dB in the frequency range of up to 4.75 GHz. The $|S_{11}|$ dependence resonance at a frequency of 5 GHz is determined by the length and width of the regular part of the enclosure (Fig. 7 *a*). According to the results of optimizing a model with a rectangular case, the $|S_{11}|$ maximum value does not exceed minus 28 dB for a frequency of 4.8 GHz (Fig. 7 *b*). Moreover, the latest model provides $|S_{11}|$ with a level of no more than minus 30 dB in the frequency band of up to 5.3 GHz (Fig. 7 *c*).

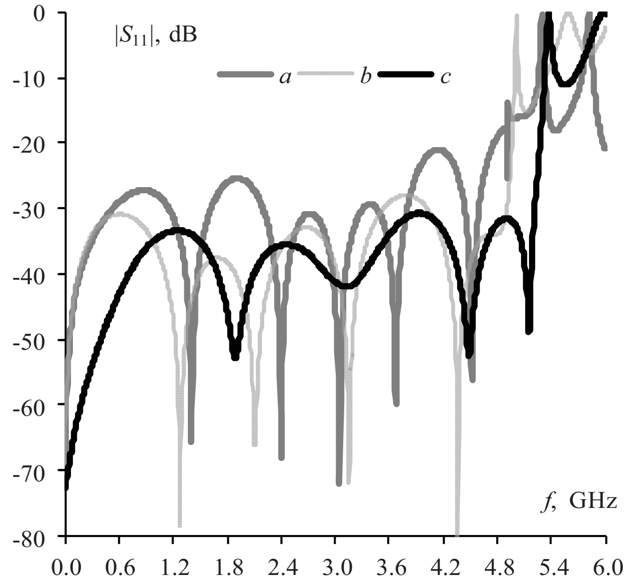

Fig. 7. Frequency dependences of $|S_{11}|$ of TEM cell models with pyramidal transitions (*a*), rectangular enclosure (*b*), tapering transitions at a constant height of the enclosure (*c*).

For further development, we selected the latest cell model which provides the best matching with a 50 Ohm path comparing with the structures analyzed. To confirm the convergence of the results obtained, a repeated electrodynamic analysis was performed with the reduced mesh size by finite element method (FEM) and transmission line matrix method (TLM). The mesh step was set by the number of sub-intervals per wavelength near the model (first index) and at the boundary of the space volume analyzed (second index) (Fig. 8). The analysis of the results revealed the identical behavior of the $|S_{11}|$ dependences obtained using two numerical methods.

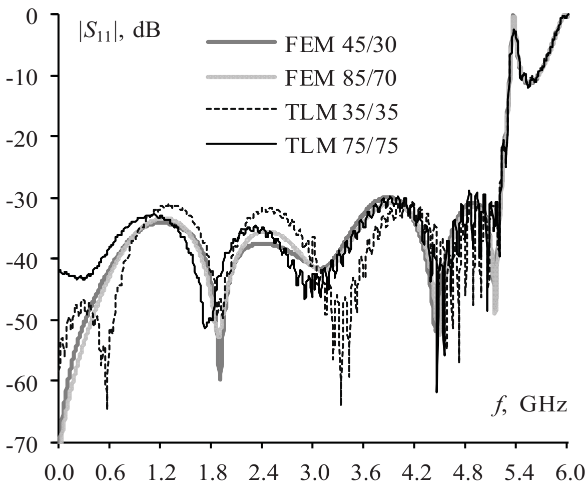

Fig. 8. Frequency dependencies of $|S_{11}|$ of the TEM cell models obtained using the TLM and FEM with reduced mesh size.

V. Development Of Research Prototype

Based on the results of electrodynamic simulation, a solid model of the TEM cell was developed, which took into account tolerances for the manufacture of elements. To install the connectors and the central conductor, it was necessary to have access to the internal space of the TEM cell; therefore, the case was divided into two parts connected by means of a mechanical screw connection. Also, the solid model takes into account the specific features of the cell assembly: the way the connectors are mounted on the enclosure and soldered with the central conductor, as well as the mounts for clamps that provide electrical metallization contact on the test PCB with the cell enclosure (Fig. 9).

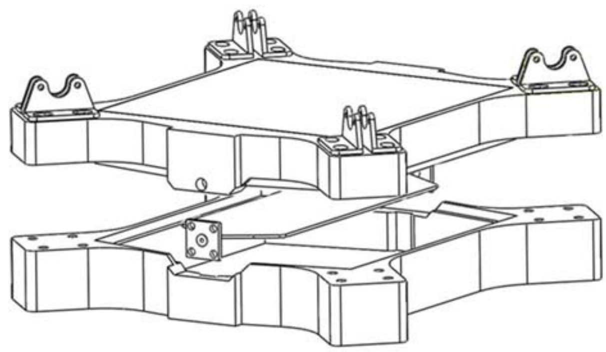

Fig. 9. Isometric view of a solid model of the TEM cell.

Fig. 10 shows the developed research prototype of the TEM cell made by milling aluminum plates and water-jet cutting of a copper sheet. To be protected against corrosion, the central conductor is coated with silver, and the remaining structural elements are coated with nickel. The *S*-parameters of the research prototype were measured using the P4M-18 vector network analyzer manufactured by Micran (Fig. 11).

Fig. 10. The research prototype of the TEM cell without a test table.

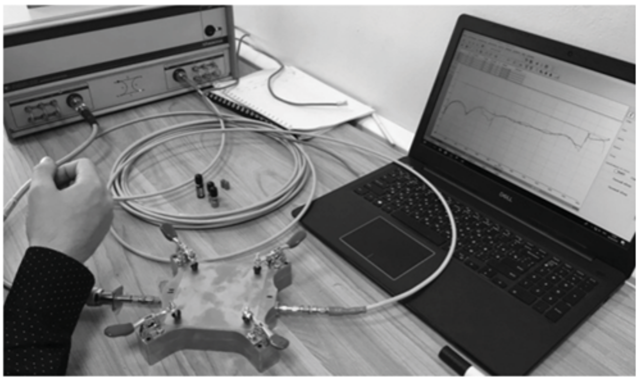

Fig. 11. Testing of the research prototype.

The frequency dependencies of $|S_{11}|$ for electrodynamic, solid models and the research prototype of the TEM cell are shown in Fig. 12. From the results obtained, it can be seen that a change in the geometric parameters of the solid model due to the permissible accuracy of the milling machine during manufacture led to an increase in the $|S_{11}|$ maximum value to the level of minus 20 dB in the operating frequency range of up to 5.3 GHz, while for the electrodynamic model this value does not exceed the level of minus 28 dB. According to the measurements of the research prototype, $|S_{11}|$ does not exceed minus 17 dB, which is acceptable for testing in accordance with standards [7, 8].

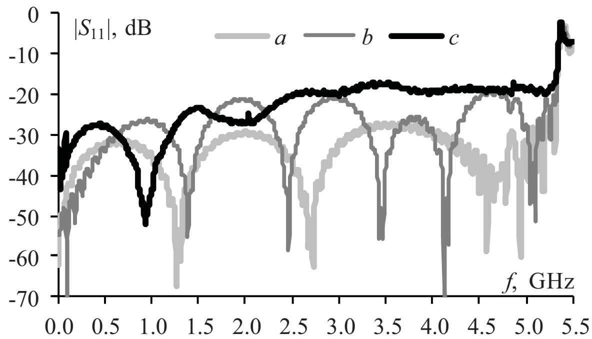

Fig. 12. Frequency dependences of $|S_{11}|$ for electrodynamic (*a*), solid (*b*) models and the research prototype (*c*) of the TEM cell.

VI. CONCLUSION

The results of developing a TEM cell for testing ICs on EMC are presented. The geometric parameters of the regular section of the TEM cell were calculated and options for matching it with a 50 Ohm path were considered. The electrodynamic analysis and parametric optimization of various models of matching transitions were performed in order to minimize the maximum value of the frequency dependence of the reflection coefficient $|S_{11}|$ in the range of operating frequencies. Based on the calculated electrodynamic and developed solid models, the research prototype of the TEM cell was manufactured and proved suitable for studying and testing ICs with a profile height of no more than 5 mm for electromagnetic emission and radiated immunity. The measurements of the research prototype showed the maximum value of $|S_{11}|$ minus 17 dB in the operating frequency range of up to 5.3 GHz.

ACKNOWLEDGMENT

The research was carried out at the expense of Russian Science Foundation grant 19-79-10162 in TUSUR.

REFERENCES

[1] T.N. Theis and H.-S. P. Wong, “The end of Moore's law: a new beginning for information technology”, Computing in science & engineering, vol. 19, no. 2, pp. 41-50, Mar. 2017.
[2] F.L. Fiori, “Investigations on the susceptibility of smart power ICs to RFI”, Proc. International symposium on electromagnetic compatibility, pp. 743-747, Sept. 2013.
[3] Yu.A. Pirogov and A.V. Solodov, “Damages of integrated microcircuits in radio fields”, Journal of radio electronics, no. 6, 2013.
[4] N.V. Baljuk et al, “Moshhnyj jelektromagnitnyj impul's: vozdejstvie na jelektronnye sredstva i metody zashhity”, Moscow: Gruppa IDT, 2008, 478 p.
[5] A.V. Klyuchnik et al. “Methodical aspects of the IC stability studies in pulse RF electromagnetic fields”, Journal of radio electronics, no. 8, 2010.
[6] Integrated circuits – Measurement of electromagnetic immunity 150 kHz to 1 GHz – Part 4: Direct RF power injection method, IEC 62132-4, 2006.
[7] Integrated circuits – Measurement of electromagnetic emissions, 150 kHz to 1 GHz – Part 2: Measurement of radiated emissions, TEM cell and wideband TEM cell method, IEC 61967-2, 2005.
[8] Integrated circuits – Measurement of electromagnetic immunity – Part 2: Measurement of radiated immunity, TEM cell and wideband TEM cell method, IEC 62132-2, 2010.
[9] B. Mohajer-Iravani and O.M. Ramahi, “Reactive power radiated from the planar electromagnetic bandgap structures a source of EMI in high speed packages”, Proc. of the IEEE International symposium on antennas and propagation, pp. 1840-1843, 2011.
[10] M.L. Crawford, “Generation of standard EM fields using TEM transmission cells”, IEEE Transactions on electromagnetic compatibility, vol. 16, no. 4, pp. 189-195, Nov. 1974.
[11] C.M. Weil, “The characteristic impedance of rectangular transmission lines with thin center conductor and air dielectric”, IEEE Transactions on microwave theory and techniques, vol. 26, no. 4, pp. 238-242, Apr. 1978.
[12] M.L. Crawford et al, “Expanding the bandwidth of TEM cells for EMC measurements”, IEEE Transactions on electromagnetic compatibility, vol. 20, no. 3, pp. 368-375, Aug. 1978.
[13] M.E. Komnatnov and T.T. Gazizov, “Optimizatsiia geometricheskikh parametrov TEM-kamery”, Tekhnologii elektromagnitnoi sovmestimosti, vol. 59, no. 4, pp. 7-16, 2016.
[14] X. Miao and Z. Liu, “An adaptive retrospective trust region method for unconstrained optimization”, Proc. International conference on information science and engineering, pp. 1-4, 2010.
[15] A.V. Demakov and M.E. Komnatnov, “Improved TEM-cell for EMC tests of integrated circuits”, Proc. International multi-conference on engineering, computer and information sciences, pp. 399-402, 2017.
[16] A.V. Demakov and M.E. Komnatnov, “Development of a TEM-cell for electromagnetic compatibility testing of integrated circuits”, Doklady TUSUR, vol. 21, no. 1, pp. 52-56, 2018.

Alexander V. Demakov was born in in 1994. He graduated from the TUSUR in 2018. Currently, he is a PhD student at TUSUR and works as a junior researcher at the Research Laboratory «SECRF». The field of scientific interests is developing EMC test facilities.

Maxim E. Komnatnov was born in 1987. He graduated from the TUSUR in 2013 and defended his PhD thesis. Currently, he works as a senior researcher at the Research Laboratory «SECRF» and an associate professor at the Department of Television and Control at TUSUR. The field of scientific interests includes measurements and tests on EMC. M.E. Komnatnov is the author and coauthor of 106 scientific papers.